PERGAMON

Journal of Structural Geology 23 (2001) 67–80

JOURNAL OF STRUCTURAL GEOLOGY

www.elsevier.nl/locate/jstrugeo

Quartz plastic segregation and ribbon development in high-grade striped gneisses

J. Hippertt[a,*], A. Rocha[a], C. Lana[b], M. Egydio-Silva[c], T. Takeshita[d]

[a]*Departamento de Geologia, Universidade Federal de Ouro Preto, 35400-000, Ouro Preto, MG, Brazil*
[b]*Impact Cratering Research Group, Geology Department, University of Witswatersrand, Wits P.O. 2050, Johannesburg, South Africa*
[c]*Instituto de Geociências, Universidade de São Paulo, 05422-970, São Paulo, SP, Brazil*
[d]*Department of Earth and Planetary Systems Science, Hiroshima University, 739, Higashi-Hiroshima, Japan*

Received 23 August 1999; accepted 21 July 2000

Abstract

Quartz microstructures and *c*-axis fabrics formed during development of polycrystalline quartz ribbons in striped gneisses from the high-grade Além Paraíba shear zone, in southeastern Brazil, are documented. Cluster analysis of quartz grains in samples exhibiting different degrees of shear strain revealed that formation of ribbons was a mass conservative process, where isolated quartz grains became plastically segregated and then coalesced to form polycrystalline ribbons. These ribbons are separated by feldspar-rich domains devoid of quartz. The stage at which individual, stretched quartz grains start to contact each other and initiate ribbon development represents a crucial microstructural change from single grain to polycrystalline ribbon deformation mode, which is reflected by an abrupt increase in the smoothness of the ribbon boundaries. This change is interpreted to represent a strain-softening kink in the stress-strain-time path. Progressive ribboning is accompanied by strengthening of the *c*-axis fabric *Z*-maximum, indicative of continued plastic flow by basal $< a >$ glide. Operation of basal $< a >$ glide at these high-temperature conditions (680–700°C) is interpreted to be a consequence of relatively dry deformation conditions. A model is then proposed for development of straight quartz ribbons in high-grade striped gneisses, where scattered quartz grains are continuously stretched and segregated by crystal–plastic processes. The small angle misorientation of the contacting grains enables subsequent coalescence and resulting grain size enlargement. Pervasive grain boundary migration accounts for the straight grain boundaries and rectangular grain shapes within the ribbons.

1. Introduction

Development of elongate polycrystalline quartz aggregates (Type B quartz ribbons of Boullier and Bouchez, 1978) is a common feature in gneisses subjected to predominant shear deformation at upper amphibolite to granulite facies metamorphic conditions (e.g. Culshaw and Fyson, 1984; McLelland, 1984; Mackinnon et al., 1997). The presence of these ribbons characterizes the high-grade striped gneisses, originally described by Lehmann (1884) in the granulitic terrain of Saxony (Spry, 1969). This type of polycrystalline ribbon is typically only one grain wide, and comprises an aggregate of rectangular/sub-rectangular quartz grains whose grain boundaries are straight, oriented parallel and perpendicular to the ribbon contacts. Typical grain size is in the order of a few to several hundred micrometers. A strong preferred crystallographic orientation is generally present in the form of a single girdle with maximum parallel to *Y* (e.g. McLelland, 1984; Mackinnon et al., 1997) or *Z*-axis of finite strain (this paper). Some fabrics can also show maxima in an intermediate position between *Y* and *Z*. A main characteristic in all of these ribbon-bearing gneisses is that almost all the quartz within the rock is concentrated in the ribbons, which are separated by feldspar-rich domains nearly devoid of quartz. The bulk rock composition (varying between alkali–granitic and granodioritic), however, is generally very constant and independent of the degree of ribboning. This fact indicates that formation of quartz ribbons was most likely a mass conservative process, where significant introduction of silica from an external source did not occur. Microstructures indicative of crystal-plastic deformation such as deformation bands and subgrains are relatively scarce in these ribbons, compared with the situation in other ribbons and quartz veins deformed at lower metamorphic grade conditions (e.g. Takeshita and Hara, 1998). This is a consequence of the thermal energy available at high-grade conditions, which allows recovery/recrystallization of quartz to proceed at faster rates through grain boundary migration such that intracrystalline deformation microstructures are obliterated

* Corresponding author.

0191-8141/01/$ - see front matter
PII: S0191-8141(00)00129-2

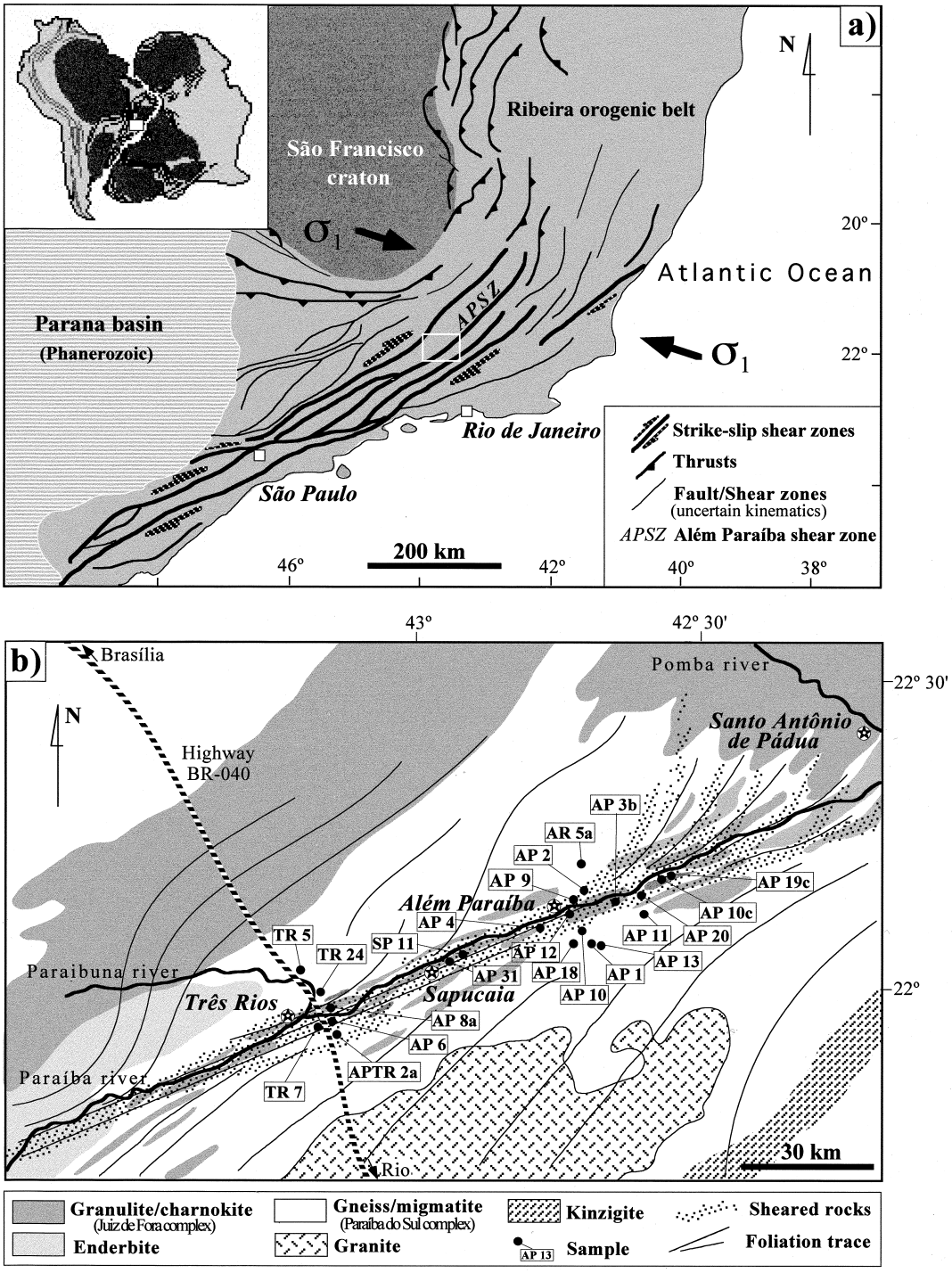

Fig. 1. (a) Map showing the major thrusts and strike-slip ductile shear zones of the Pan-African-Brasiliano Ribeira orogenic belt (0.8–0.6 Gyr) in southeastern Brazil. The main compressive stress (σ_1) is also indicated as determined by the orientation of mechanical twinning in plagioclase (modified from Egydio-Silva and Mainprice, 1999). The boxed area is shown in 'b'. (b) Map showing the main rock units and sample location in the studied sector of the Além Paraíba shear zone near Três Rios, Sapucaia and Além Paraíba towns, Rio de Janeiro State.

(Urai et al., 1986). Different grain sizes, grain morphologies and deformation microstructures in these ribbons are interpreted to reflect different conditions of temperature, strain rate and extent of post-deformational annealing (Boullier and Bouchez, 1978).

Previous work on ribbon-bearing high-grade gneisses (e.g. Culshaw and Fyson, 1984; McLelland, 1984) have interpreted straight quartz ribbons as result of deformation of pre-existing quartz layers or other types of quartz aggregates. They assume, therefore, an initial compositional

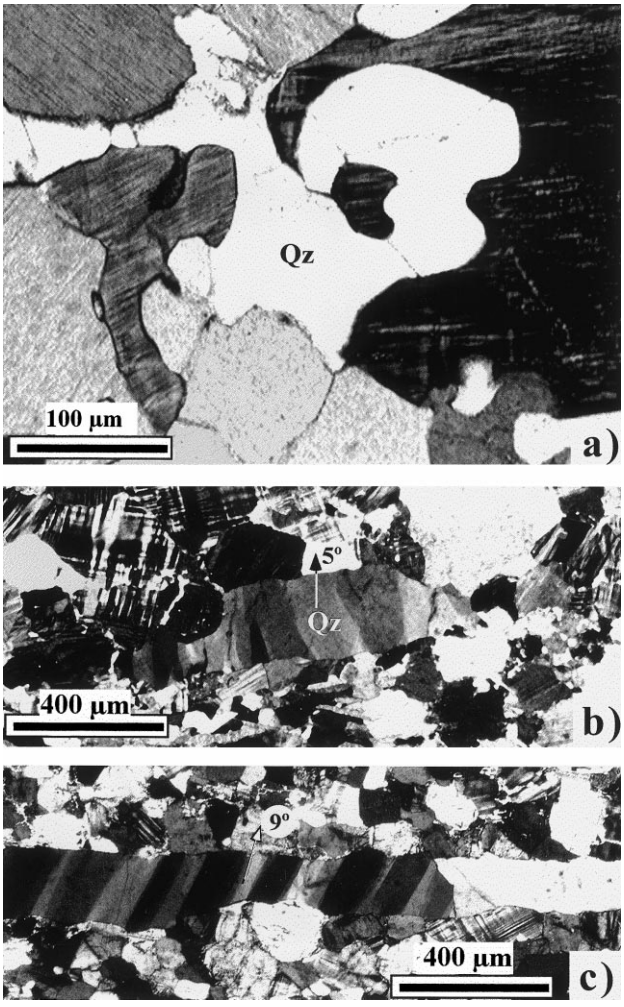

Fig. 2. (a) Microstructure of a regional high-grade gneiss of the Paraíba do Sul Complex outside the shear zone, showing interstitial quartz between recrystallized feldspar grains (Sample AP-13). (b) Elongated quartz grain from a low strain domain in the margin of the shear zone (sample APTR-2a). Quartz shows deformation bands oriented at a low angle to the *c*-axis trace (arrow) and high angle to the longest grain axis. (c) Straight quartz ribbon in a high strain domain of the shear zone (Sample AP-12) showing deformation bands sub-parallel to [*c*] and oriented at a high angle to the *X*-axis of finite strain, suggesting crystal-plastic deformation through basal $<a>$ slip. All photos taken on *XZ* thin sections (PPL).

anisotropy that preceded formation of straight ribbons. Alternatively, Mackinnon et al. (1997) has proposed a fracture model for quartz ribbons, based on the straight contacts of quartz with bordering non-quartz grains that suggest they were truncated. In their model, migration of silica is attributed to water-assisted diffusion through grain boundaries.

In this paper, we investigated progressive development of quartz ribbons in regional gneisses from the Proterozoic Ribeira fold belt of southeastern Brazil, during deformation in the high-grade Além Paraíba shear zone. Finely layered striped gneisses were formed in the shear zone domains, where quartz ribbons are noticeably developed. A representative microstructure of these high-grade striped gneisses is shown in Passchier and Trouw (1996, fig. 5.10, p. 107). By means of a microstructural clustering analyses, a transitional stage is documented wherein deformed quartz grains contact each other and coalesce, initiating formation of polycrystalline ribbons. A new formation mechanism is proposed whereby quartz is continuously segregated by plastic flow into shear plane-parallel ribbons during progressive deformation.

2. Geological setting

2.1. Regional geology

The Além Paraíba shear zone is a deep-crustal, transcurrent shear zone formed in a high-temperature/low-pressure high-grade terrain which is well exposed throughout SE of Minas Gerais and NE of Rio de Janeiro states, in southeastern Brazil (Fig. 1a). This high-grade terrain constitutes the basement of the Ribeira fold belt (Juiz de Fora and Paraíba do Sul complexes) which records an early granulite facies metamorphism at 2220 ± 27 Ma (Söllner et al., 1991). These rock units have been intensively reworked by tectonic, magmatic and metamorphic processes during the last important orogenic event (0.8–0.6 Gyr Pan-African-Brasiliano orogeny) in this region, with development of several mylonite zones which are typically ~10–15 km-wide. These mylonite zones contain pervasive *S–C* fabrics and also exhibit a well-defined *S–C* geometry over a scale of several hundred kilometers, which is consistent with the pervasive dextral shear sense recorded in most individual mylonite zones (Hippertt, 1999).

The Além Paraíba shear zone is one of these mylonite zones (Fig. 1b). It is a 10 km-wide, at least 400 km-long, strike-slip vertical shear zone occurring in the north-central portion of Rio de Janeiro State. Geothermometric/geobarometric calculations based on microprobe analysis (Porcher et al., 1995; Fernandes et al., 1996) indicated that temperatures during deformation varied between 680–750°C (hornblende–garnet–biotite), and pressure between 5-7 kbar (garnet–plagioclase–biotite–quartz–sillimanite). Both temperature and pressure increase northwards.

The sheared gneisses within the Além Paraíba shear zone display a conspicuous millimetric–centimetric straight layering in *XZ* sections that is parallel to both the shear zone walls and the compositional gneissic banding of decimetric–metric scale. This layering represents the vertical/sub-vertical mylonitic foliation present along the entire shear zone. On the plane of the mylonitic foliation, there is a conspicuous horizontal to shallowly plunging lineation defined by alignment of amphibole crystals, feldspar porphyroclasts and the quartz ribbons focussed on in this paper. Foliation inflections in the shear zone limits (Fig. 1b) as well as asymmetrically mantled feldspar porphyroclasts and, more locally, oblique shape fabrics defined by some

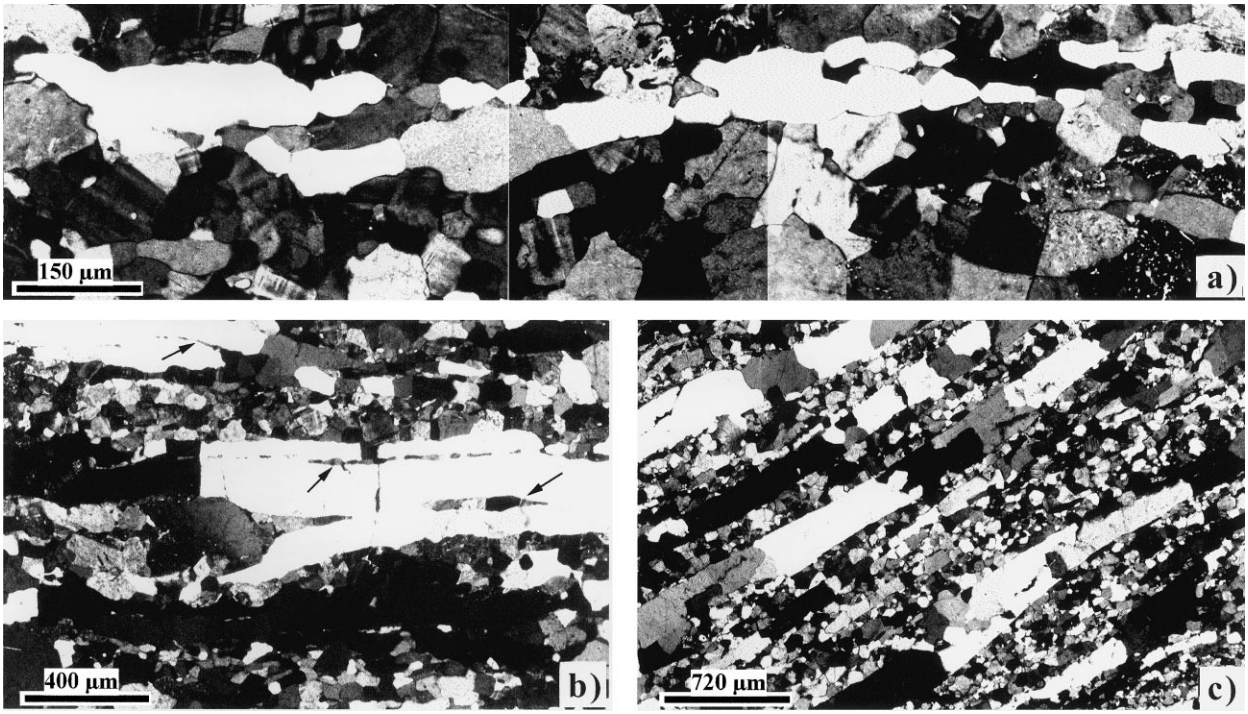

Fig. 3. (a) Quartz ribbon in initial stage of development from a low/moderate strain domain of the shear zone. Note that the elongate quartz grains start to contact each other (and coalesce) in the *X* direction (sample AP-10, clustering number = 0.97). (b) Well-developed polycrystalline ribbons surrounding a larger feldspar grain (*F*). The limited coalescence in the *Z* direction is reflected by the profusion of discontinuous, elongate feldspar aggregates (arrows) between the individual ribbons (sample AP-9). (c) Typical microstructure of the striped gneisses in domains of high shear strain. Quartz occurs as straight, polycrystalline ribbons separated by layers of recrystallized feldspar devoid of quartz (sample TR-7).

quartz ribbons consistently indicate an overall dextral shear sense in this shear zone.

2.2. Regional high-grade rocks

The regional high-grade rocks are represented by banded gneisses, migmatites and different types of granulites of the Juiz de Fora complex. Away from the shear zone, all of these rock types show a centimetric–metric compositional banding with varied proportions of quartz, feldspar and mafic minerals (hornblende and biotite, mainly). Sillimanite and garnet are important in the peraluminous metasedimentary gneisses. Feldspar phenocrysts are common in the more granitic lithotypes, varying from 0.5 to 5 cm in diameter. Dark hornblende crystals, ranging from 1 mm to 2 cm in diameter, are common (1–10%). Some migmatites occur interbedded with the gneissic compositional banding. These migmatites have a granitic/alkali–granitic composition (K-feldspar and quartz are the main constitute minerals) and show veined, stromatic and schlieren structures. Migmatite occurrences are generally parallel to the gneissic banding, with their dimensions varying from a few to several meters.

In thin section, the regional gneisses display a typical granoblastic texture defined by polygonal aggregates of plagioclase and K-feldspar (grain size 150–250 μm) with slightly curved or straight grain boundaries and without any preferred shape orientation, except for hornblende and biotite crystals and some elongate quartz crystals. K-feldspar and, more rarely, plagioclase may occur as porphyroclasts showing deformation bands and incipient core-and-mantle microstructures. Most quartz crystals occur between polygonal feldspar grains forming monocrystalline interstitial pockets or aggregates of a few crystals (Fig. 2a).

2.3. Sheared gneiss

Within the shear zone, the mylonitic gneisses are characterized by eye-shaped plagioclase and K-feldspar porphyroclasts (1–5 cm in diameter) with well-developed core-and-mantle microstructures, surrounded by a matrix of recrystallized polygonal feldspar (grain size 100–400 μm) where plagioclase shows strong lattice preferred orientation with (010) subparallel to the regional foliation and an [*a*] maximum parallel to *Y* (Egydio-Silva and Mainprice, 1999). Quartz occurs in the form of straight, mono and polycrystalline ribbons 100 μm to 2 mm wide that can reach up to several centimeters in length (Fig. 2b,c). These ribbons occur along the mylonitic foliation (*C*-planes) or, locally, as sigmoidal lenses that inflect around large feldspar porphyroclasts and define discrete oblique *S*-planes. Biotite platelets are connected to each other, forming continuous folia that anastomose around the feldspar porphyroclasts.

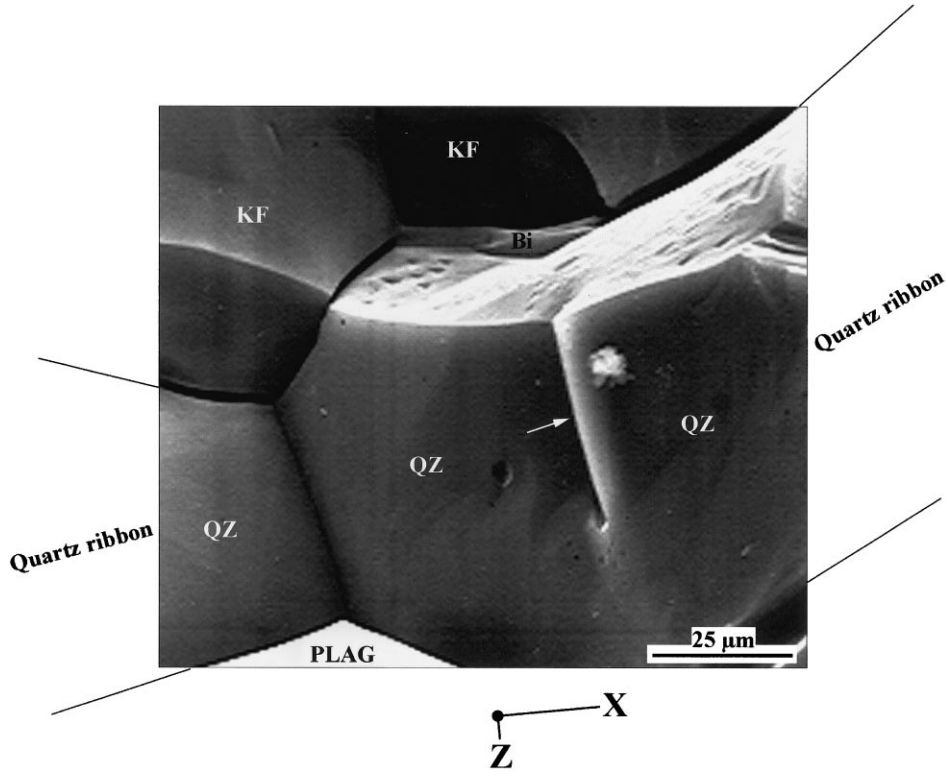

Fig. 4. SEM observation of an artificially produced intergranular fracture surface in sample AP-10, showing an incipient polycrystalline quartz ribbon (QZ) with a planar discontinuity (arrow) oriented at high angle to the ribbon maximum dimension (*X* direction). This feature is interpreted as a partially healed, relic grain boundary between two coalesced quartz grains. View sub-parallel to lineation and perpendicular to foliation. SEM settings: SE mode, 30 kv, carbon–gold coating. Mineral identification made through EDS analysis. K-feldspar (KF), Plagioclase (PLAG).

Hornblende is less common in the sheared gneiss than in its precursor outside the shear zone. High strain domains are generally mica-poor and consist of finer grained (60–120 μm) recrystallized feldspar and quartz ribbons, with rare feldspar porphyroclasts. These domains show a very straight milimetric–submilimetric layering defined by alternating quartz ribbons and layers of recrystallized feldspar devoid of quartz (Fig. 3c).

3. Microstructural analysis

3.1. Quartz microstructure: general description

Outside the shear zone, quartz occurs as homogeneously distributed individual grains (100–400 μm) or aggregates of a few grains which are equant to slightly elongate, devoid of deformation bands, and typically occupy irregular interstices between feldspar grains with straight or slightly curved grain boundaries (Fig. 2a). Proximal to the shear zone, the individual quartz grains lose their interstitial character, become more elongate, with smoother boundaries and increasingly stronger undulose deformation bands. These deformation bands are regularly shaped and sized in *XZ* sections, and display sharp boundaries oriented at high angle to the *X* morphological grain axis (Fig. 2b), as also occur in the straight polycrystalline ribbons in the high strain domains of the shear zone (Fig. 2c).

The transition from low/moderate to high strain domains in the shear zone is marked by a stage where the individual elongate quartz grains contact each other and incipient ribbons are formed (Fig. 3a). This stage corresponds to the disappearance of feldspar porphyroclasts, which are replaced by aggregates of polygonal grains, reflecting the complete recrystallization of feldspar. SEM observation of these incipient polycrystalline ribbons revealed some planar discontinuities interpreted as partially healed grain boundaries of adjacent quartz grains (Fig. 4). With increasing strain, the polycrystalline ribbons become progressively more continuous and straighter, in parallel with grain size reduction in the feldspar aggregates (Fig. 3b,c).

3.2. c-Axis fabrics, fabric intensity and deformation bands

Two sets of thin sections were made from 23 selected samples whose location are shown in Fig. 1. One set is perpendicular to the foliation and parallel to lineation (interpreted as parallel to the *XZ* finite strain plane), and another is perpendicular to both foliation and lineation (interpreted as parallel to the *YZ* finite strain plane). Determinations of *c*-axis fabrics were made with a Leitz 5 axes universal stage in all the *XZ* thin sections. Most fabrics are *YZ* single

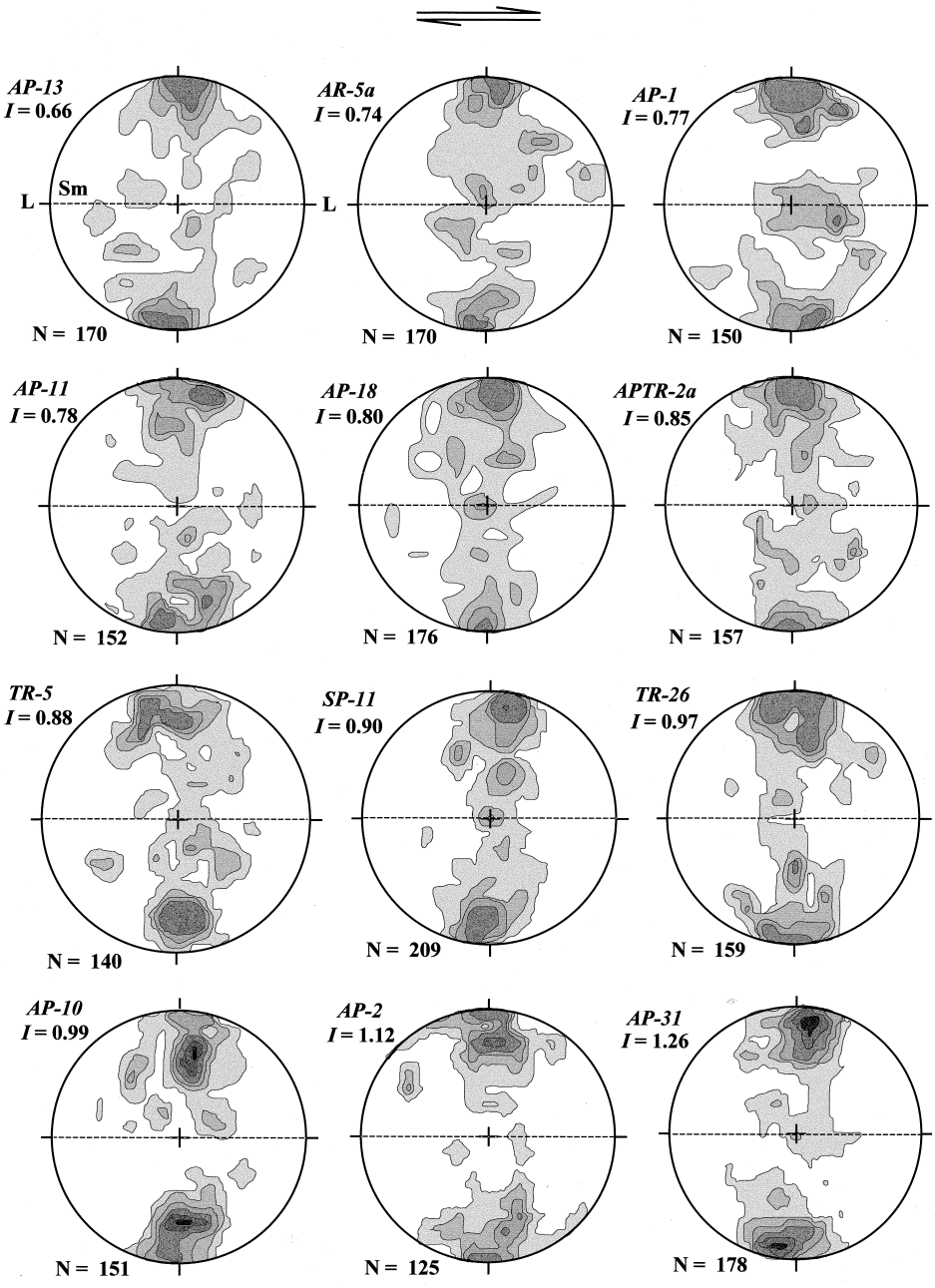

Fig. 5. *c*-Axis fabrics of samples without ribbons or with ribbons in initial development stage. Fabrics are ordered by increasing fabric intensity (*I*). Ribbons start to form from sample AP-10 ($I = 0.99$) onwards. Note that the maximum strength suddenly increases from this sample onwards. Density contours are 1%/1% area. Foliation (Sm) is vertical, lineation (L) is horizontal E–W in all diagrams. Equal area lower hemisphere projection.

girdles with a small asymmetry relative to the foliation plane, where the girdles are generally rotated clockwise by 0–10° about the *Y*-axis (Figs. 5 and 6). This asymmetry is nearly always consistent with the overall dextral shear sense of the shear zone. In the most common situation, *c*-axes define maximum concentrations close to the *Z*-axis of finite strain, but maxima close to *Y*, or in intermediate positions between *Y* and *Z* also occur in other samples, which were not included in this study. The presence of these *Y* and intermediate maxima is generally associated with partially melted domains (migmatites) where abundant quartzo–feldspathic veins are associated with the tectonites. Because the comparison between intensities of fabrics with different skeletons is generally not feasible (Woodcock, 1977), and also to avoid the effects of melt on the evolving microstructure, we have restricted our analyses of fabric intensities and microstructures to the case where *c*-axis maximum close to *Z* occurs. Therefore, all our data refer to the 23 selected samples where *Z*-maxima occur.

An attempt was made to correlate the development of crystallographic preferred orientation with quartz ribboning. The fabric intensity is calculated based on eigenvalues of

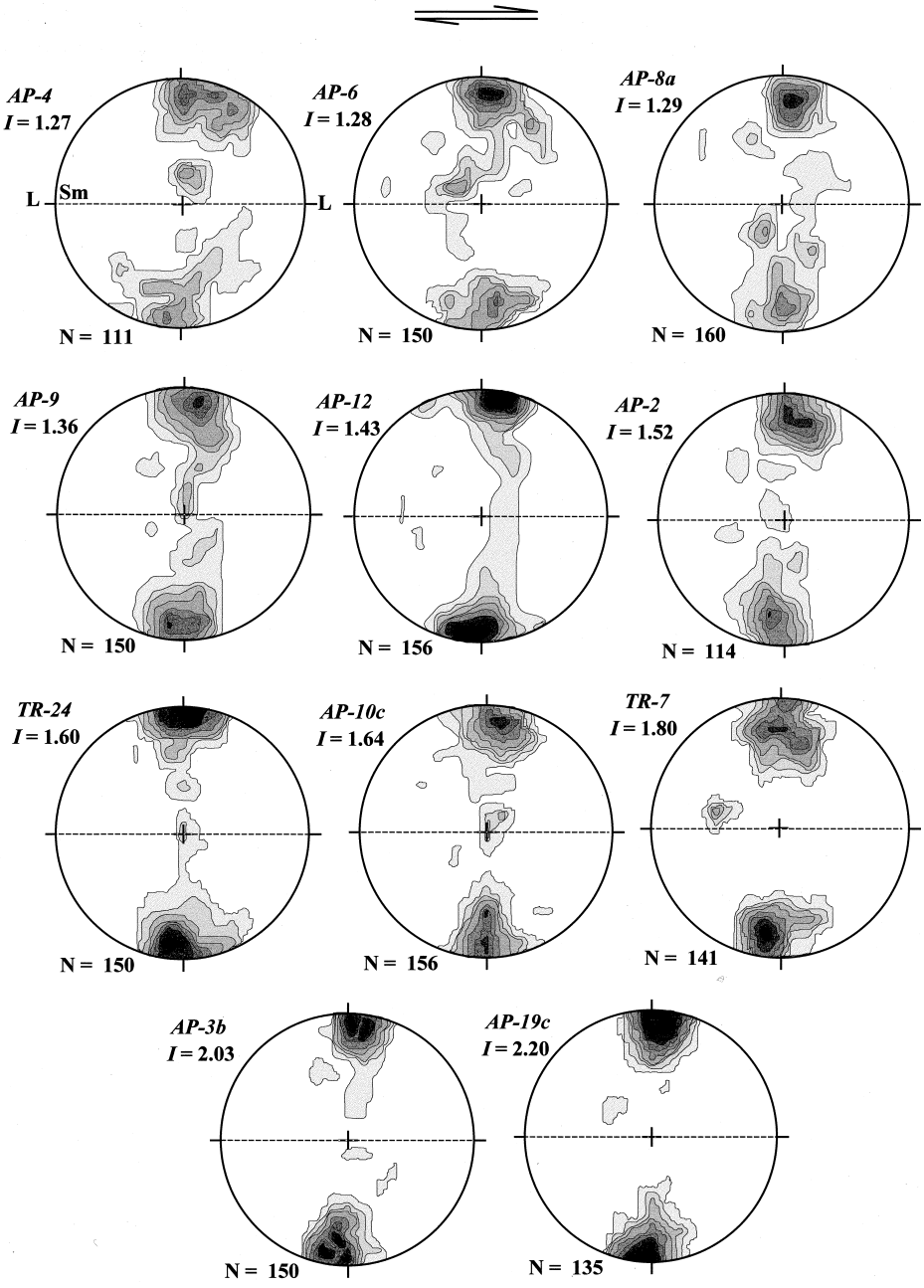

Fig. 6. *c*-Axis fabrics of samples from moderate- to high-strain domains showing well-developed polycrystalline quartz ribbons. Fabrics are ordered by increasing fabric intensity (*I*). Density contours are 1%/1% area. Foliation (Sm) is vertical, lineation (L) is horizontal E–W in all diagrams. Equal area lower hemisphere projection.

orientation tensors S_i $(i = 1,2,3)$ of *c*-axis fabrics (Woodcock, 1977), where the fabric intensity I (Lisle, 1985) is given by:

$$I = 7.5 \sum_{i=1}^{3} (S_i - 1/3)^2. \quad (1)$$

The distribution of maxima and submaxima in *c*-axis fabric skeletons formed by simple shear directly reflects the glide systems operative during deformation, where the slip plane tends to approach the bulk shear plane; and the slip direction the bulk shear direction (e.g. Law et al., 1990). Intracrystalline slip is also reflected in the orientation of deformation bands (undulose extinction bands), where the band boundaries are oriented at high angles to the slip direction and the slip plane. By using the gypsum plate, the obliquity of the deformation band boundaries relative to the *c*-axis trace in *XZ* thin sections was determined to serve as an additional check on the inferences about operative glide systems made from the *c*-axis fabrics (Fig. 7). Both *c*-axis maximum orientation and deformation band

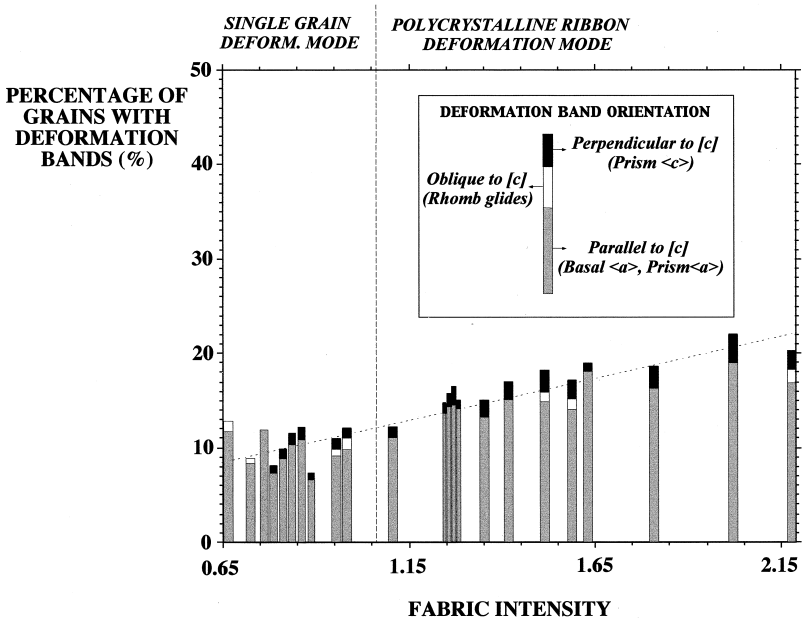

Fig. 7. Diagram showing variation of deformation band orientation relative to the *c*-axis trace, as observed in *XZ* thin sections ordered by increasing fabric intensity (horizontal axis).

orientation are consistent with a predominant basal $< a >$ slip in all of the samples.

3.3. Clustering analysis

Clustering analysis is a useful tool for microstructural investigation (Srivastava and Isaaks, 1993) but, for the purpose of this study, common clustering methods based on variations of the distance to the nearest grain were not effective to describe the quartz spatial distribution in these rocks. This is because the quartz distribution changes progressively from a pattern of scattered, isolated grains to large, discrete ribbons, where grain size differences of more than one order of magnitude exist. To follow the progressive deformation and redistribution of quartz in the shear zone, we have investigated the clustering pattern of quartz in both *XZ* and *YZ* sections of all selected samples by attributing a clustering index to each individual quartz grain, intercepted in randomly chosen profiles across the thin sections (Fig. 8). The clustering index chosen was the number of quartz grains in contact with the intercepted grain. From 50 to 120 intercepted grains were computed in each section, from which an average clustering index was calculated. Although individual clustering indices vary between 0 (for totally isolated grains) to a number generally smaller than 6, the average clustering index for an entire thin section (referred to as *clustering number*) is much more limited (between 0 and 2) and reflects well the evolving quartz distribution with progressive ribboning. No significant differences were observed between clustering numbers from *XZ* and *YZ* sections. Therefore, the clustering numbers used in this paper are averages of *XZ* and *YZ* values. Clustering numbers smaller than 0.5 were obtained in samples where most quartz grains are isolated and still preserve an interstitial character. The clustering number approaches 1 when individual grains are elongated and, sometimes, contact each other. Incipient polycrystalline ribbons occur in these samples (e.g. Fig. 3a). Clustering numbers between 1 and 2 were obtained in samples where well-defined one-crystal-wide polycrystalline ribbons predominate (e.g. Fig. 3b,c).

3.4. Grain boundary orientation and grain boundary smoothness

Orientation of quartz grain boundaries relative to the rock foliation were determined in randomly oriented profiles across the *XZ* thin sections. The variation of grain boundary orientation reflects directly the stretching and progressive straightness of individual grains and polycrystalline ribbons. The grain boundary orientations clearly change from a homogeneous pattern to a bimodal distribution with progressive ribboning (Fig. 9).

The relative smoothness of quartz grain boundaries was determined based on the variation of grain boundary orientation. This is an important characteristic of high-grade quartz ribbons, very straight grain boundaries having been interpreted to reflect an origin by fracture infilling (Mackinnon et al., 1997). To compare the smoothness of quartz boundaries in rocks with different degrees of quartz ribbon development, and to compare this variation with other microstructural parameters, the average smoothness (F) of quartz grain boundaries for each *XZ* section was

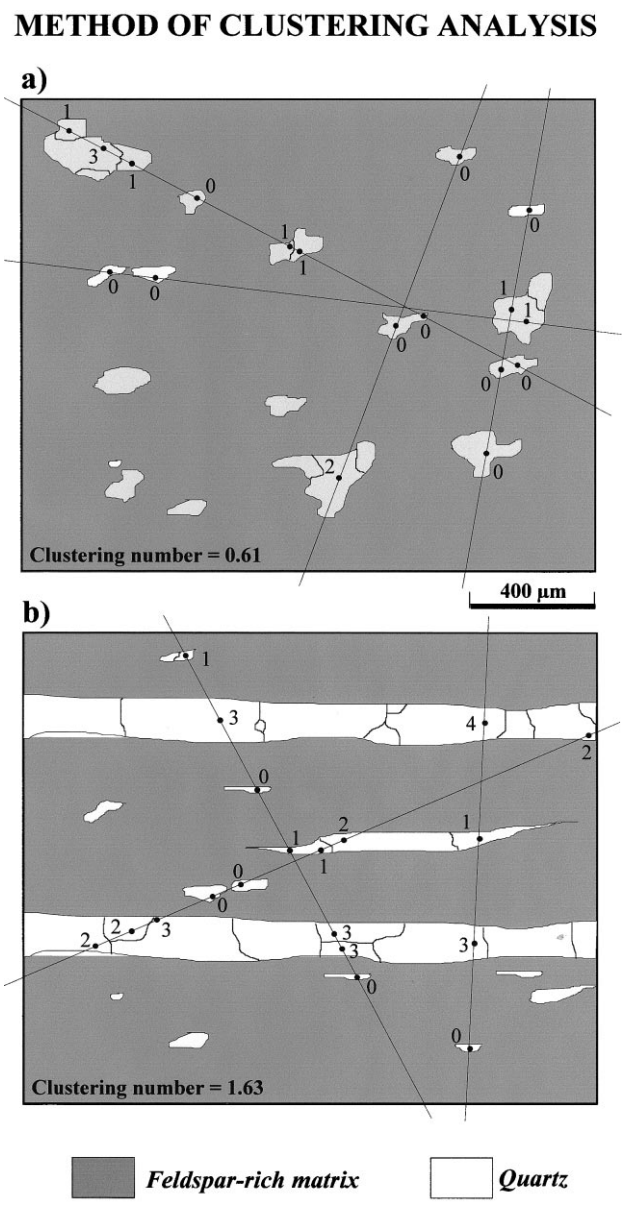

Fig. 8. Sketch illustrating the utilized method of clustering analysis where the determined "clustering number" represents the average number of quartz grains in contact with quartz intercepted in random chosen profiles through the thin-sections. (a) Microstructure of a relatively undeformed protolith outside the shear zone displaying disseminated, isolated quartz grains. (b) Microstructure of sheared striped gneisses with quartz concentrated in polycrystalline ribbons.

determined, based on variation of grain boundary orientation, by using the expression:

$$F_{(\%)} = \left(1 - \left(\sum_{\alpha=1}^{n} [\sin\alpha]/n\right)\right).100 \quad (2)$$

where α is the angle to foliation, and n is the number of grain boundaries computed. This parameter is plotted in the ratio diagrams of Figs. 10 and 11.

3.5. Quartz modal content, distribution and grain size

X, *Y* and *Z* morphological axes of 100 grains were directly measured in all *XZ* and *YZ* thin section (Fig. 11). The overall content of quartz in the samples was determined through modal analyses in *XZ* and *YZ* thin sections, and was taken the average of these two values. The distribution of quartz between matrix (i.e. individual grains occurring in the recrystallized feldspar-rich matrix) and polycrystalline ribbons was also measured. The results show a decreasing amount of matrix quartz in concert with ribbon development (Fig. 12).

3.6. Data analysis

All the measured microstructural parameters were plotted against fabric intensity (Fig. 10) and clustering number (Figs. 11 and 12). In all the diagrams, a distinction is made between *single grain* deformation mode and *polycrystalline ribbon* deformation mode, where this transition corresponds to a microstructure where individual quartz grains come into contact and incipient ribbons are developed (e.g. Fig. 3a). This transition corresponds to a quartz clustering number close to 1. All microstructural parameters (except *c*-axis fabric intensity) show an abrupt kink at this transition from single grain to polycrystalline ribbon deformation mode. In order to plot the best-fit curves for each microstructural parameter in the ratio diagrams, we have obtained correlation coefficients (R^2) for two different situations: (1) considering all the database for single grain and polycrystalline ribbon deformation modes as a single group and (2) splitting the database in two separate groups, one for each deformation mode. The curves which appear in the ratio diagrams are those which showed the highest correlation coefficients. For all parameters, except fabric intensity, the best correlation was obtained by separating the data, where different curves are defined for each deformation mode. The correlation between fabric intensity and clustering number, however, showed the best-fit curve when all data were considered, i.e. no kink occurring in the transition from single grain to polycrystalline ribbon deformation mode (Figs. 10 and 11).

4. Discussion

4.1. Ribbon development

Grain size of quartz is larger within the sheared gneisses than in the precursor rocks outside the shear zone. As temperature was roughly the same in and out of this 10-km-wide shear zone, as inferred by the same stable metamorphic paragenesis, it is concluded that coalescence of adjacent grains with low-angle lattice misorientation was important for grain size enlargement in the shear zone. Grain size enlargement due to coalescence is a common feature in polycrystalline aggregates with a strong lattice

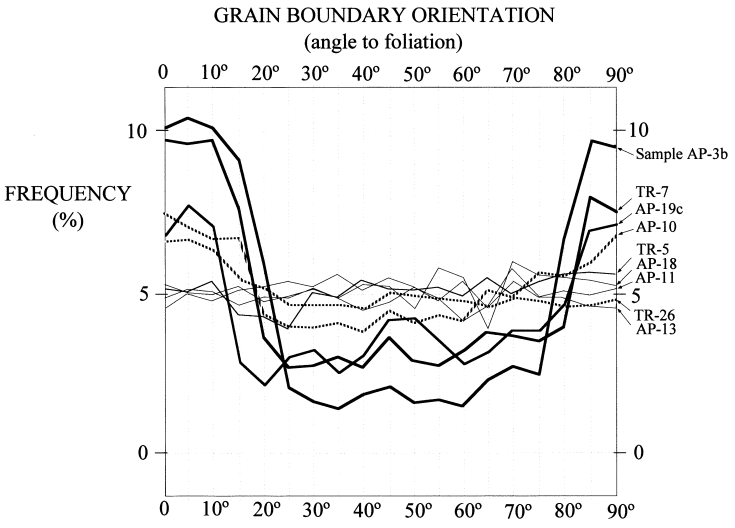

Fig. 9. Histogram showing variation of quartz grain boundary orientation in nine samples with different degrees of shear strain and ribbon development. Thin lines show a homogeneous quartz grain boundary distribution in samples with very small shear strain (samples AP-18, AP-11, AP-13, TR-5). Thicker lines, which show a bimodal distribution, are from samples with well-developed ribbons from high strain domains of the shear zone (samples AP-3b, TR-7, AP-19c). Dashed lines are from samples with low/moderate shear strain and intermediate stage of ribbon development (samples AP-10, TR-26).

preferred orientation (e.g. Herwegh and Handy, 1996). However, the results show that grain size enlargement was more pronounced for *X* than for the *Y* and *Z* morphological grain axes (Fig. 11). This indicates that grain coalescence occurred predominantly through elimination of the short grain boundaries (i.e. those parallel to the Z morphological axis) oriented at high angles to foliation (Fig. 4), and that lateral coalescence by elimination of the larger grain boundaries oriented at low angles to foliation was less common. This is interpreted to be a consequence of the

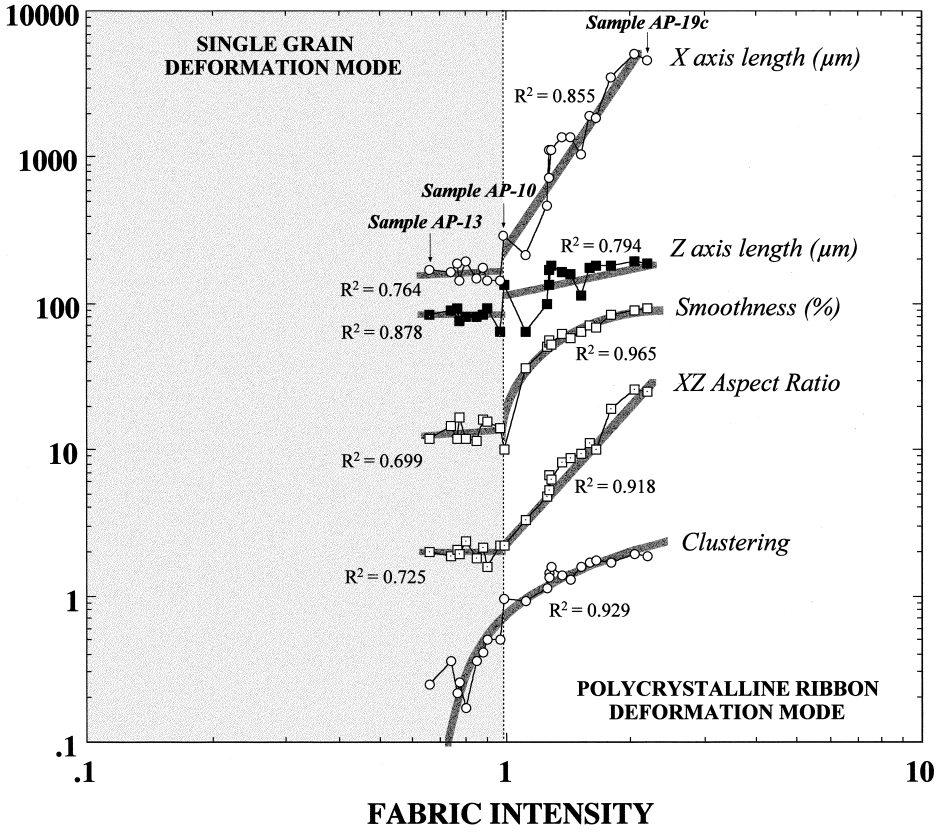

Fig. 10. Ratio diagram of *c*-axis fabric intensity vs. clustering number, grain boundary smoothness, grain dimensions and *XZ* aspect ratio of quartz.

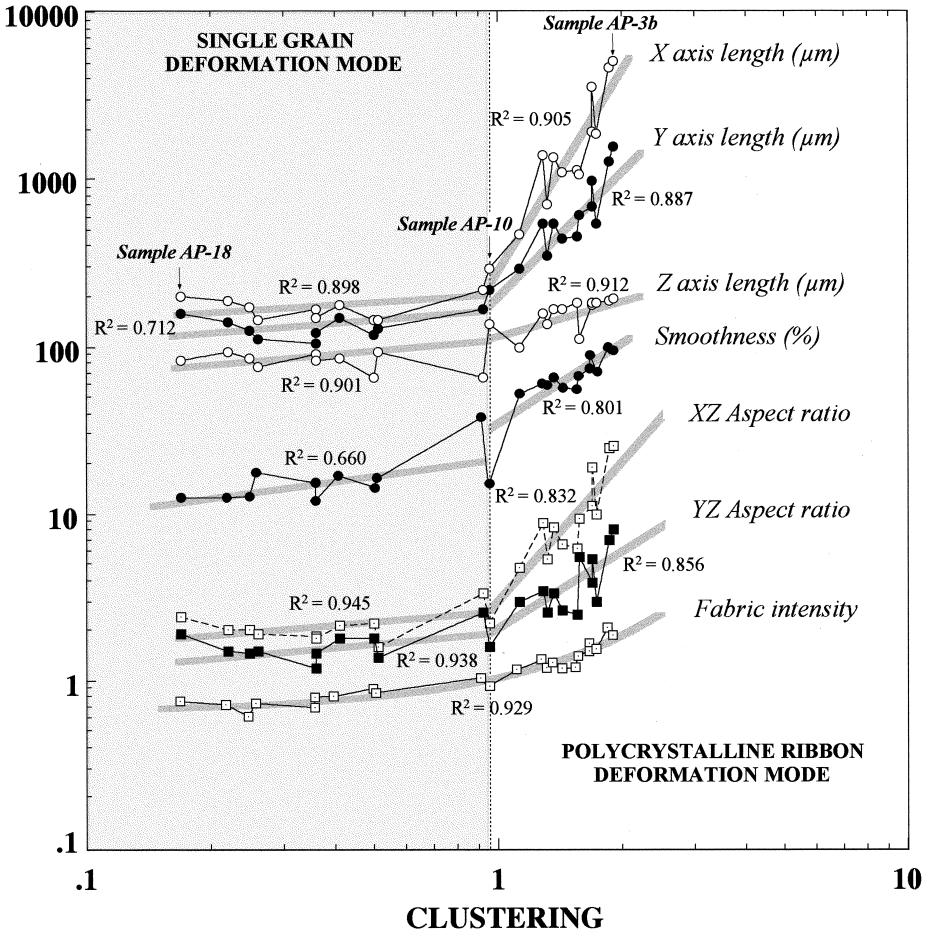

Fig. 11. Ratio diagram of clustering number vs. *c*-axis fabric intensity, grain boundary smoothness, grain dimensions and *XZ* and *YZ* aspect ratios of quartz.

elongation of quartz grains in the *X* direction through intracrystalline plasticity, as indicated by the strong *c*-axis fabrics. This process should reduce the distance to the nearest grain at faster rates along *X* than along *Y* and *Z* and, consequently, favor preferential grain coalescence in the *X* direction (Fig. 13). Nevertheless, it is also necessary to consider that grain size of the deformational microstructure was probably obliterated by post-deformational annealing, as a consequence of pervasive grain boundary migration, which typically occurs in the high-grade metamorphic environment. The large grain size, therefore, is interpreted to reflect both preferential grain coalescence in the *X* direction as well as selective grain growth by grain boundary migration. These processes are also suggested to account for the characteristic rectangular shape of quartz grains within these ribbons.

The results in Figs. 10–12 show an abrupt kink in most microstructural parameters when the clustering number approaches 1. This transition corresponds to a change from isolated grains to polycrystalline ribbon deformation mode as a result of quartz segregation and subsequent coalescence. This is suggested to represent a major change in the evolving microstructure, reflected by a strain-softening kink in the stress-strain-time path. The 'softening effect' results from the switch from a load-bearing framework microstructure, where the rheology of the aggregate is controlled by the rheology of the stronger phase (feldspar), to a layered microstructure, where the rheology of the weaker phase (quartz) is prevailing (Handy, 1990). Formation of quartz ribbons in the sheared gneisses was a mass conservative process for silica on the thin section-scale, as indicated by the nearly constant modal quartz content in all samples, aside from the progressive depletion of quartz in the matrix and associated segregation into ribbons (Fig. 12). This process led to formation of a layered structure with a resulting strain softening effect which is reflected by the abrupt increase in the smoothness of quartz aggregates when the clustering number approaches 1, i.e. after polycrystalline ribbons start to form (Fig. 11). This change is in part a simple geometrical effect of coalescence which makes many grain boundaries oriented at high angles to the *X*-axis of finite strain disappear, such that a more limited range of grain boundaries will produce smaller smoothness values, as determined by equation (2). The ribbon boundaries rapidly but, progressively, acquire a very straight character after ribboning and quartz segregation start (Fig. 3). This straightness of the ribbon boundaries led Mackinnon et al. (1997) to interpret their ribbons to be products of infilling of dilatant

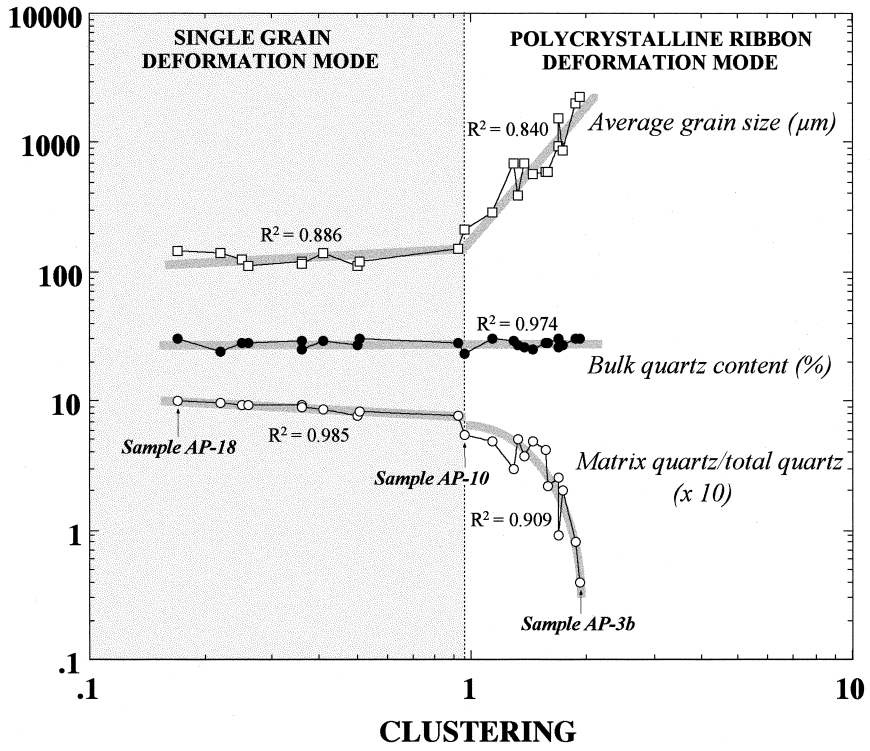

Fig. 12. Ratio diagram of clustering number vs. bulk modal quartz content, average quartz grain size and proportion of matrix quartz.

fractures (see Section 4.3). However, development of straight boundaries between rheologically contrasting layers is indeed a universal feature in tectonites which is enhanced with increasing finite strain and higher strength contrast between the adjacent domains (Berthé et al., 1979). At low metamorphic grade conditions, these straight, rheologically contrasting interfaces may evolve into discontinuities (shear fractures) in high strain domains of shear zones (e.g. Hippertt and Tohver, 1999), where a part of the strain can be accommodated through slip on the layer boundaries. However, the occurrence of fracturing is more difficult to assure in the striped gneisses focussed on in this study. This is principally due to the fact that the feldspar layers present between the quartz ribbons are also totally recrystallized and lacking porphyroclasts, which suggest pervasive crystal-plasticity and a relative low strength contrast (<10) between quartz and feldspar during deformation at these high-grade conditions (Carter and Tsenn, 1987; Handy, 1990).

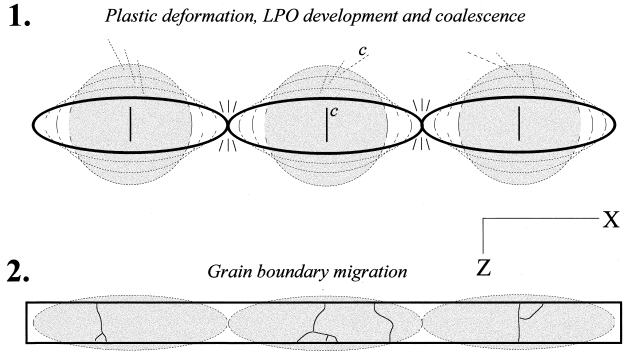

Fig. 13. Idealized sketch illustrating the proposed model for development of polycrystalline quartz ribbons in high-grade striped gneisses. In stage 1, plastic deformation of quartz through basal $<a>$ glide causes LPO development that allows lattice coalescence when isolated grains contact each other. In stage 2, pervasive grain boundary migration works to smooth grain boundaries and produce straight polycrystalline ribbons with rectangular grains.

4.2. Significance of c-axis fabrics

It is an interesting fact that the softening effect indicated by the kink in most microstructural parameters plots is not reflected in the *c*-axis fabric intensity, the only microstructural parameter where the complete data set (from single grains and polycrystalline ribbons) is best fitted by an uninflected curve (Figs. 9 and 10). This means that the rate of plastic strain of quartz was not altered after the switch from single grain to polycrystalline ribbon deformation mode, and that the *c*-axis fabric intensity increased uninterruptedly relative to strain and clustering number. This is an expected situation during deformation at temperatures higher than 650°, i.e. close to the melting temperature of quartz, where dislocation creep is maximized and prevents work hardening (Hirth and Tullis, 1992). As a consequence, an ideal orientation with the operative slip plane oriented at low angles to the shear plane (maximum RSS on the slip plane) can be produced with relatively low

finite strains, as indicated by the relatively strong *c*-axis fabrics, even outside the shear zone. A similar scenario is also indicated by the domainal *c*-axis fabrics shown by Mackinnon et al. (1997); fig. 5) where matrix and ribbon quartz show the same *c*-axis preferred orientation. This evolving *c*-axis fabric pattern, however, contrasts radically with the common situation in low-temperature, greenschist facies tectonites, where the crystallographic preferred orientation of quartz abruptly strengthens after segregation and foliation development take place, suggesting a softening effect due to enhanced crystal-plasticity (e.g. Handy, 1990; fig. 2).

The pattern of *c*-axis close to the foliation plane (*Z*-maximum) indicates that basal $<a>$ slip was the main operative glide in the investigated samples (e.g. Law et al., 1990). This is not the common situation in other documented occurrences of ribbon-bearing high-grade gneisses where the presence of a strong *Y*-maximum is more common (e.g. McLelland, 1984; Mackinnon et al., 1997), and reflects dominant prism $<a>$ glide during deformation of quartz at high temperature (Schmid and Casey, 1986). Although *Y*-maximum and intermediate maxima between *Y* and *Z* (potentially indicative of rhomb $<a>$ glides) do exist in the Além Paraíba shear zone, we have observed a clear spatial association of these fabrics with the presence of partially melted domains where abundant quartzo–feldspathic veins occur. In contrast, the samples with *Z*-maximum investigated in this paper came from outcrops where migmatization during shearing did not occur or was only incipient. We have concentrated our investigation in the latter samples to permit an evaluation of the fabric intensity with progressive ribboning, and also to avoid the effects of melt on the evolving microstructure. This relationship between *Y*-maximum and migmatites (whose occurrence may reflect the presence of an aqueous fluid phase) is consistent with the idea that the transition from basal $<a>$ to both prism $<a>$ and prism $<c>$ glides could be associated not only with temperature, but mainly with an hydrolytic weakening effect due to water diffusion along [*c*] (Blacic, 1975; Linker et al., 1984).

4.3. Alternative hypothesis

Previous work in striped gneisses containing polycrystalline quartz ribbons has proposed that these one crystal-wide ribbons result from progressive deformation of preexisting quartz-rich domains (Boullier and Bouchez, 1978; McLelland, 1984; Culshaw and Fyson, 1984) or infilling of dilatant fractures (Mackinnon et al., 1997). The crucial observation in this study is the clear transition from a microstructure with scattered matrix quartz in the regional gneisses outside the shear zone, to a ribbon-bearing microstructure whose development increases with strain in the shear zone. Our results show that ribbon development was a mass process accompanied by progressive quartz depletion in the matrix and formation of a deformational rock anisotropy (due to quartz mobilization), and not the result of superimposed deformation of a pre-existing compositional anisotropy.

The fracture model of Mackinnon et al. (1997) is, among other things, based on the straightness of quartz ribbons and truncation of adjacent feldspar grains. To check if their hypothesis would be feasible in the Além Paraíba occurrence, we have compared the aspect ratio of feldspar grains from different domains relative to the quartz ribbons limits in three samples (AP-12, AP-19c, AP-3b) where ribbons are conspicuously developed. The *XZ* aspect ratio of feldspar grains varies between 1 and 1.6 with no difference being noted between grains that are or are not adjacent to quartz ribbons, as would be expected to occur if these grains were fractured. Also, no match of feldspar grains were found across the quartz ribbons, as would occur at least in some cases if the ribbon limits represent fracture walls. The straightness of the ribbons is not a supporting argument in this case, as this microstructural characteristic was shown to *progressively* increase with quartz segregation and ribbon development, a situation that is not consistent with an origin via fracturing and vein infilling. The smoothness of quartz ribbons, therefore, is suggested to be caused by diffusion creep through phase boundaries, which is common in high-grade quartzo–feldspathic rocks (e.g. Gower and Simpson, 1992) and reflects an energetically economic geometry of lowest surface energy between adjacent domains of contrasting rheologic properties. Both quartz and feldspar aggregates are products of pervasive crystal-plastic deformation and associated recrystallization during deformation at high-grade conditions, where grain boundary migration driven by differences in grain boundary energy typically produces straight grain boundaries.

5. Conclusions

Quartz microstructures and *c*-axis fabrics in the Além Paraíba shear zone support the following conclusions with respect to formation of straight polycrystalline quartz ribbons in striped gneisses from high-grade shear zones:

1. Straight quartz ribbons develop progressively by continued crystal-plastic deformation of scattered quartz grains, which acquire a strong preferred orientation with relatively low degrees of shear strain. As a consequence, the small misorientation of adjacent grains allows coalescence when neighboring grains contact each other after some stretching in the *X*-direction of finite strain.
2. The contact and coalescence of individual, stretched quartz grains is a major microstructural change marked by a switch from single grain to polycrystalline ribbon deformation mode. This switch reflects the development of a rheologically layered rock with alternating quartz ribbons and feldspar-rich layers devoid of

quartz, and corresponds to a strain-softening kink in the stress-strain-time path.

3. The larger grain size of quartz relative to the undeformed precursor outside the shear zone, the straight grain boundaries and the characteristic rectangular shape of quartz in these one-grain-wide ribbons is a consequence of both grain coalescence and enhanced grain boundary mobility in the high-grade metamorphic environment.

Acknowledgements

Financial support for this research was provided by the Brazilian National Research Council (CNPq, process 523688/96-2).

References

Berthé, D., Choukroune, P., Jegouzo, P., 1979. Orthogneiss, mylonite and non-coaxial deformation of granites: the example of the South Armoricain shear zone. Journal of Structural Geology 1, 31–42.

Blacic, J., 1975. Plastic deformation mechanisms in quartz: the effect of water. Tectonophysics 2, 171–194.

Boullier, A.-M., Bouchez, J.-L., 1978. Le quartz en rubans dans les mylonites. Bulletin of the Geological Society, France 7, 253–262.

Carter, N., Tsenn, M., 1987. Flow properties of continental lithosfere. Tectonophysics 136, 27–63.

Culshaw, N., Fyson, W., 1984. Quartz ribbons in high grade gneiss: modifications of dynamically formed quartz c-axis preferred orientations by oriented grain growth. Journal of Structural Geology 6, 663–668.

Egydio-Silva, M., Mainprice, D., 1999. Determination of stress directions from plagioclase fabrics in high grade deformed rocks (Além Paraíba shear zone, Ribeira Fold belt, southeastern Brazil). Journal of Structural Geology 21, 1751–1772.

Fernandes, L., Porcher, C., Egydio-Silva, M., Vauchez, A., 1996. Structural evolution and temperature conditions along a high-grade shear zone in SE Brazil. International Conference on Structure and Properties of High Strain Zones in Rocks, Verbania, Italy (September 3-7). Abstract Volume, Universita di Milano Ricerca Scientifica, Supplemento 107, 61.

Gower, R., Simpson, C., 1992. Phase boundary mobility in naturally deformed, high-grade quartzfeldspathic rocks: evidence for diffusional creep. Journal of Structural Geology 14, 301–314.

Handy, M., 1990. The solid-state flow of polymineralic rocks. Journal of Geophysical Research 95, 8647–8661.

Herwegh, M., Handy, M., 1996. The evolution of high temperature mylonitic microfabrics: evidence from simple shearing of a quartz analogue (norcamphor). Journal of Structural Geology 18, 689–710.

Hippertt, J., 1999. Are *S-C* structures, duplexes, and conjugate shear zones different manifestations of the same scale-invariant phenomenon? Journal of Structural Geology 21, 977–986.

Hippertt, J., Tohver, E., 1999. On the development of zones of reverse shearing in mylonitic rocks. Journal of Structural Geology 21, 1603–1614.

Hirth, G., Tullis, J., 1992. Dislocation creep regimes in quartz aggregates. Journal of Structural Geology 14, 145–149.

Lehmann, J., 1884. Untersuchungen über die Entstehung der allkristallinen Shiefergesteine im Sächsischen Granulitgebirge. Bonn, 1884.

Law, R., Schmid, S, Wheeler, J., 1990. Simple shear deformation and quartz crystallographic fabrics: a possible natural example from the Torridon area of NW Scotland. Journal of Structural Geology 12, 29–45.

Linker, M., Kirby, S., Ord, A., Christie, J., 1984. Effects of compression direction on the plasticity and rheology of hydrolytically weakened synthetic quartz crystals at atmospheric pressure. Journal of Geophysical Research 89, 4241–4255.

Lisle, R., 1985. The use of the orientation tensor for the description and statistical testing of fabrics. Journal of Structural Geology 7, 115–117.

Mackinnon, P., Fueten, F., Robin, P.-Y., 1997. A fracture model for quartz ribbons in straight gneisses. Journal of Structural Geology 19, 1–14.

McLelland, J., 1984. The origin of ribbon lineation within the southern Adirondacks, U.S.A. Journal of Structural Geology 6, 147–157.

Passchier, C., Trouw, R., 1996. Microtectonics. Springer-Verlag, Berlin.

Porcher, C., Fernandes, L., Egydio-Silva, M., Vauchez, A. 1995. Dados preliminares do metamorfismo M1 da Faixa Ribeira: Região de Três Rios e Santo Antônio de Pádua (RJ). V Simpósio de Estudos Tectônicos, Gramado, RS, Brazil, Boletim de Resumos, 71-73.

Schmid, S., Casey, M., 1986. Complete fabric analysis of some commonly observed quartz *c*-axis patterns. American Geophysical Union Geophysical Monography 36, 263–286.

Söllner, F., Lammerer, B., Weber-Diefenbach, K., 1991. Die krustenentwicklung in der küstenregion nördlich von Rio de Janeiro/Brasilien. Münchner Geologische Helfe 4, 1–101.

Spry, A., 1969. Metamorphic Textures. Pergamon Press, Oxford.

Srivastava, R., Isaaks, E., 1993. An Introduction to Applied Geostatistics. Oxford University Press, Oxford.

Takeshita, T., Hara, I., 1998. c-Axis fabrics and microstructures in a recrystallized quartz vein deformed under fluid-rich greenschist conditions. Journal of Structural Geology 20, 417–431.

Urai, J., Means, W., Lister, G., 1986. Dynamic recrystallization of minerals. In: Hobbs, B., Heard, H. (Eds.), Mineral and Rock Deformation: Laboratory Studies. American Geophysical Union, Geophysical Monograph, pp. 61–99.

Woodcock, N., 1977. Specification of fabric shapes using an eigenvalue method. Geological Society of America Bulletin 88, 1231–1236.